

CdSeS/ZnS Alloyed Nanocrystal Lifetime and Blinking Studies under Electrochemical Control

Wei Qin, Raman A. Shah, and Philippe Guyot-Sionnest*

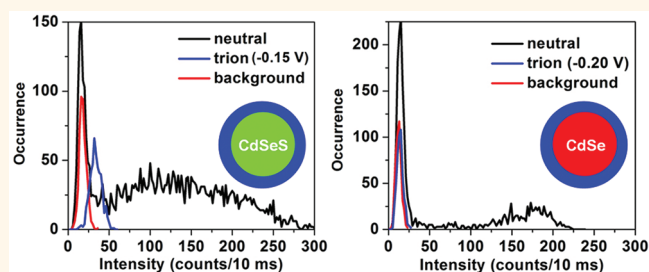
James Franck Institute, 929 E. 57th Street, The University of Chicago, Chicago, Illinois 60637, United States

Core/shell semiconductor nanocrystals exhibit bright and stable luminescence¹ and are finding applications in imaging^{2,3} and displays.^{4,5} However, single QD studies have unveiled unusual blinking statistics^{6,7} which is an active topic of discussion today.⁸ To broaden the applications of the materials, small, nonblinking, and widely tunable nanocrystals are sought. In recent years, blinking has been essentially suppressed by using thick CdS shells on CdSe,^{9,10} but at the cost of large size and vanishing electron confinement energy. Alternatively, rather small CdZnSe alloyed nanocrystals have been reported to exhibit no blinking,¹¹ but the study has not been corroborated.

The first interpretation of the blinking phenomenon was that a photoionization event leads to a delocalized charge inside a dot, which then, *via* an Auger-like process, leads to fast nonradiative recombination of further photogenerated excitons until ejection or trapping of the charge.^{12,13} While it has been directly confirmed that charged QDs are dimmer than neutral QDs,¹⁴ further experiments showed that charged dots emit at a level that is too high to explain the dark state in single QD blinking.^{15,16} Therefore, the dark state of blinking dots remains a subject of speculation.

Nevertheless, charged QDs are indeed dimmer rather than neutral dots because of Auger relaxation. Reducing the Auger rate in small dots would lead to brighter charged dots for applications as potential sensors or as laser materials. The fast Auger process in CdSe QDs was first reported 20 years ago,¹⁷ and it is widely assumed that the Auger process in nanocrystals operates as in bulk semiconductors, albeit with a different rate due to the differing density of states and wave function overlap.¹⁸ Recently, Cragg and Efros showed that sharp interfacial boundaries relaxed the momentum selection rule and would facilitate

ABSTRACT



Alloyed CdSeS nanocrystals allow tuning between the CdSe and CdS band edges while remaining relatively small. The CdSeS cores also lead to a reduced electron confinement energy and a slower biexciton decay rate compared to CdSe cores of similar sizes. A ZnS shell synthesis procedure allows stable CdSeS/ZnS colloidal quantum dots (QDs) suitable for single dot imaging. These are compared to CdSe/ZnS of similar core size. The blinking off-exponents of the CdSeS/ZnS dots in air and on a glass substrate were slightly larger. Using electrochemistry with ensemble and single dot measurements, the trion lifetime of CdSeS/ZnS dot is resolved to be ~ 0.75 ns, while it is about 0.15 ns for CdSe/ZnS. In addition, the blinking behavior of single CdSeS/ZnS QDs is largely suppressed when in the trion state.

KEYWORDS: spectroelectrochemistry · alloyed nanocrystals · trion decay · biexciton decay · lifetime · blinking behavior

fast Auger recombination.¹⁹ They therefore proposed to use materials with graded interfaces, softening the confinement potential, and recent experiments on CdSe/CdS with attempts to alloy the interface showed much slower Auger relaxation.²⁰

In this work, we investigate the class of CdSeS nanocrystals.^{21,22} We develop a ZnS shell synthesis method that leads to bright and stable nanocrystals that can be tuned more widely than the CdSe/CdS systems. Recently, electrochemistry on single dots along with fluorescence detection has been demonstrated,²³ and we apply this method to learn about the photoluminescence (PL) lifetime of the charged alloyed QDs and compare the results to CdSe/ZnS QDs of similar sizes.

* Address correspondence to pgs@uchicago.edu.

Received for review November 16, 2011 and accepted December 14, 2011.

Published online December 22, 2011
10.1021/nn2044388

© 2011 American Chemical Society

RESULTS AND DISCUSSION

Growth of ZnS Shells on Alloyed CdSeS QDs. Adopting the methods from Jang,²¹ CdSeS nanocrystals were synthesized, in which a sulfur–selenium mixture dissolved in TOP was directly injected into the cadmium oleate solution at high temperature. The colloidal nanocrystals have homogeneous shape and narrow size distribution (5.0 ± 0.4 nm) (Supporting Information, Figure S1). The PL of CdSeS QDs (QY, 14%) can be easily quenched by the addition of the thiol ligand. ICP analysis shows that the molar ratio of sulfur to selenium is 5.5:1 in CdSeS QDs. The XRD measurements demonstrate that CdSeS QDs have a zinc blende structure with intermediate peaks lying between that of pure CdSe and CdS QDs (Figure 1a). This confirms that there are no separate CdSe and CdS domains in CdSeS QDs. Also, the average size of particles (5.6 ± 0.2 nm), calculated from the Debye–Scherrer formula, is consistent with that measured by TEM. The band-edge absorption energy of CdSeS QDs is 2.25 eV (Figure 1b). CdSe/CdS core/shell QDs with the same S/Se composition would have a CdSe core size of 2.8 nm and CdS shell thickness of 1.1 nm, the band-edge absorption energy of which is about 2.1 eV.^{9,24} These separate facts confirm that sulfur and selenium are alloyed in the CdSeS QDs to some degree. Furthermore, the nanocrystals may have a “gradient” structure since selenium is more reactive than sulfur to cadmium, as reported in the previous literature.^{21,22}

The growth of a ZnS shell on CdSe cores can greatly enhance the photostability of QDs because of surface passivation and increased carrier confinement.¹ The same strategy can be applied on CdSeS alloyed cores. To grow a relatively thick ZnS shell to effectively passivate a CdSe surface, a high reaction temperature in excess of 220 °C is typically necessary. However, in contrast to CdSe cores, the CdSeS alloyed cores undergo strong ripening under 220 °C, leading to a complete loss of the core spectrum and separate growth of ZnCdS nanocrystals. All initial attempts to grow the ZnS shell by utilizing the SILAR methods²⁵ at that temperature were unsuccessful (Supporting Information, Figure S2). We concluded that the alloyed nature of CdSeS cores might render the surface atoms more mobile under high temperature compared to pure CdSe cores and lead to faster dissolution. Therefore, an alternative scheme was developed to first grow one to two monolayers of a ZnS shell on the CdSeS core at a lower temperature to increase its stability followed by further deposition of ZnS under higher temperature. The formation of a ZnS shell is then accompanied by only a small red shift of the absorption and PL spectrum. Concurrently with the ZnS shell growth, the size distribution is slightly broadened (Supporting Information, Figure S1) and the PL intensity is enhanced (QY, 20%) (Figure 1b).¹ The most beneficial aspect of the ZnS shell

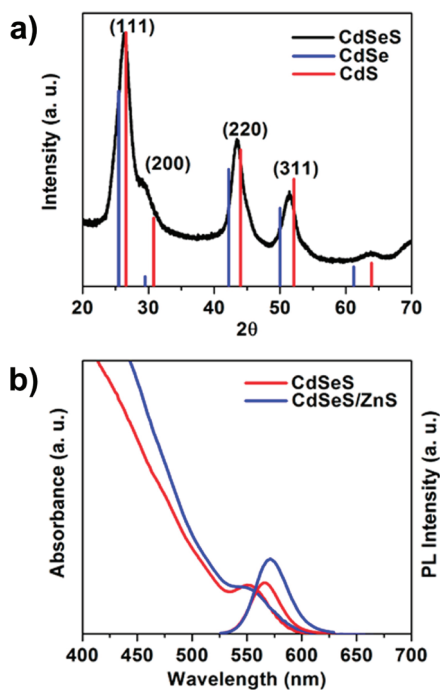


Figure 1. (a) XRD spectra of CdSeS QDs, normalized to the height of the (111) peak. The diffraction peak positions for pure CdSe and CdS nanocrystals are shown, separately. (b) Absorption and PL spectrum of CdSeS and corresponding CdSeS/ZnS alloyed nanocrystals.

is the much improved photostability under continuous illumination (Supporting Information, Figure S3).

Ensemble Measurements of CdSeS/ZnS QDs. To characterize the effects of the alloyed structure on Auger recombination, the biexciton decay was measured for CdSeS/ZnS and CdSe/ZnS samples by transient absorption pump–probe spectroscopy. The biexciton lifetimes for CdSeS/ZnS and CdSe/ZnS QDs were extracted to be 140 and 85 ps, respectively (Figure S4), corresponding to a $\sim 40\%$ reduction of the recombination rates in the alloyed dots. Therefore, although CdSeS/ZnS have a reduced rate of Auger recombination, Auger channel is not suppressed.¹⁹ The results of intraband measurements show that CdSeS alloyed cores with a 2.25 eV 1S exciton peak have a 0.20 eV $1S_e-1P_e$ intraband transition energy (Supporting Information, Figure S5). Previous work in our group showed that zinc blende CdSe QDs with the same 1S exciton peak have an intraband energy of 0.33 eV,²⁶ which also corresponds to an approximately 40% reduction in confinement energy for the CdSeS cores.

The effect of extra charges on the optical properties of CdSeS/ZnS QDs was measured by applying electrochemical control and monitoring the PL simultaneously. To mitigate the effects of energy transfer among QDs,¹⁵ a relatively dilute solution of CdSeS/ZnS was used to prepare the film such that the QDs are not close-packed but still numerous within the confocal spot. For both CdSeS/ZnS and CdSe/ZnS QDs, the PL can be quenched reversibly with the application of a

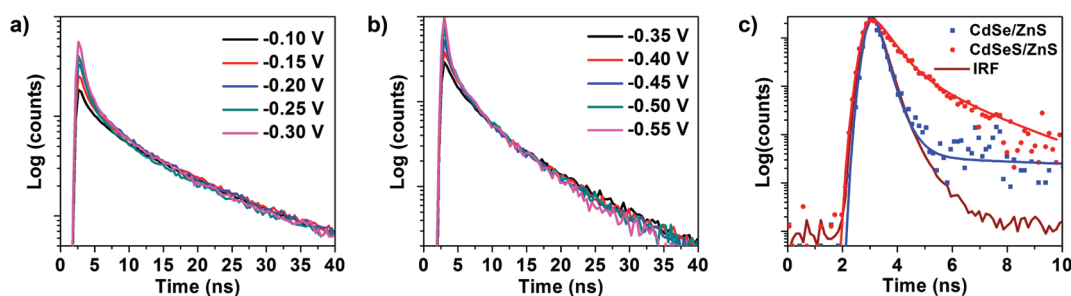


Figure 2. Normalized lifetime traces for (a) CdSe/ZnS and (b) CdSe/ZnS QDs dilute films. (c) Trion decay traces of CdSe/ZnS and CdSe/ZnS QDs, and IRF trace measured from the fast fluorescence decay of 1% picric acid. The corresponding lines of multiexponential fits are also displayed after convolution with the IRF.²⁷

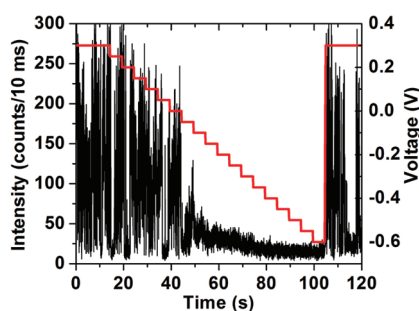


Figure 3. PL trajectory of single CdSe/ZnS dot, varying applied voltage as shown from 0.30 to -0.60 V in 50 mV steps and back to 0.3 V.

negative potential (Supporting Information, Figure S6). In addition, the lifetime traces develop a fast decay component as the negative potential is applied. After normalizing the lifetime traces at different voltage, the curves show almost indistinguishable decay for $t > 10$ ns (Figure 2a,b). Therefore, we propose that the faster component of the lifetime trace is due to the trion PL of charged QDs and the slower decay arises from the PL of neutral QDs, the relative ratio of which can be tuned by electrochemistry.¹⁵ Trion lifetime traces were obtained by subtracting the exponential trace extrapolated from long times. The trion lifetime trace of CdSe/ZnS shows a lifetime of ~ 0.15 ns,²⁷ after deconvolution of the instrument response function (IRF) measured from the fast fluorescence decay of 1% picric acid. However, CdSe/ZnS QDs shows a trion decay evidently slower, with a lifetime of ~ 0.75 ns (Figure 2c).²⁷ Therefore, we conclude that CdSe/ZnS QDs have a slower trion decay rate than CdSe/ZnS QDs, which is consistent with the slower biexciton recombination rate. We note that the trion lifetime of CdSe/ZnS QDs is longer than the biexciton lifetime by a factor of 5.

PL Measurements of Single CdSe/ZnS QDs. Emission traces for single CdSe/ZnS QDs were measured to characterize the blinking behavior of alloyed nanocrystals. Compared with CdSe/ZnS QDs, single CdSe/ZnS alloyed nanocrystal seem less frequently to have long “off” periods. However, the off-time probability distribution for single CdSe/ZnS alloyed QDs still obeys

power-law statistics^{7,8} with an average exponent of 2.1 for 20 single dots. This is a bit larger than for single CdSe/ZnS QDs (1.9) under similar conditions (Supporting Information, Figure S7). Therefore, we conclude that there is only a small difference in the blinking behavior between these two types of QDs, with the alloyed dots showing marginally reduced blinking.

Under electrochemical control, the PL response of single CdSe/ZnS dots were measured, during which an external sawtooth voltage was scanned from 0.30 V to -0.60 V in 50 mV steps lasting 5 s each and then switched directly back to 0.30 V (Figure 3). The photoluminescence was unambiguously quenched when the applied voltage was brought to -0.60 V and recovered “instantly” after the voltage was brought back to 0.30 V. This is consistent with a previous study.²³ Strikingly, the PL trace displays a steady diminution of intensity within the range from 0 to -0.35 V.

To exclude the effect of background, we applied the same analysis to photons collected from a region without QDs. It shows that the PL signal of the background remains unaffected whenever the bias is below 0 V (Supporting Information, Figure S8). Assuming that the fluorescence of the single dot is completely quenched by injection of electrons from -0.40 to -0.60 V since the PL signal changes little at this range, the signal in that range is taken as background. After background subtraction, the lifetime traces show a distinct change of shape with the appearance of a faster decay component as the voltage drops below 0 V (Supporting Information, Figure S9). From 0 V, the photon counts at early times increase, which is consistent with a faster radiative recombination associated with the formation of the singly charged trion state (Figure 4).^{15,23} In ensemble measurements, the first and second electron injections in the $1S_e$ orbital were not resolved.²⁸ In the single dot measurement, as the voltage becomes more negative, the counts at early times for the lifetime traces then decrease gradually, consistent with observed faster decay, which suggests the addition of the second electron (Supporting Information, Figure S9). Then, around -0.30 V, the PL drops as the background level, which would be consistent with further electron

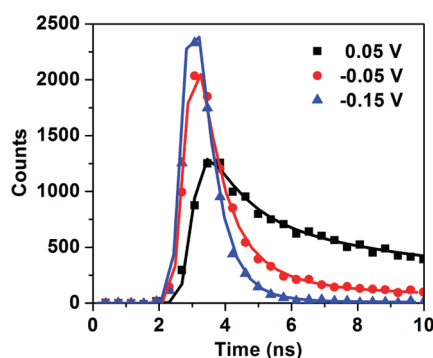


Figure 4. Lifetime traces of all photons collected at 0.05, -0.05 , and -0.15 V, after subtracting a background trace collected at -0.40 V. The global triexponential fits for the lifetime traces are also shown with the lifetimes $\tau_1 = 12$, $\tau_2 = 1.2$, and $\tau_3 = 0.5$ ns after convolution with the IRF. At different voltages, the normalized coefficients for the lifetimes are 54%, 46%, 0 at 0.05 V; 5%, 38%, 57% at -0.05 V; 0.3%, 6%, 93% at -0.15 V, respectively.

injection in the $1P_e$ state, given the 0.2 eV intraband transition energy.

The instantaneous lifetime of single dots over 50 ms bins was also extracted. The histograms of instantaneous lifetime from 0.30 to 0.05 V have a broad distribution, reflecting the blinking for neutral single dots during the binning (Figure 5).²⁹ Taking bins in which the dot is always “on”,³⁰ the radiative lifetime of single CdSeS/ZnS is 12 ns in this experiment. It is much shorter than the lifetime of single CdSeS/ZnS dots on glass (measured to be 30 ns). Using the value on glass for the radiative lifetime, and attributing the shorter lifetime on ZnO/ITO to a nonradiative energy transfer (Figure S10), the energy transfer rate is calculated to be about 0.05 ns^{-1} . As the potential is brought below 0 V, the lifetime distribution narrows and shifts to a much smaller value assigned to the trion. The lifetime distribution remains unchanged from -0.15 V to -0.25 V and thus we propose that the single CdSeS/ZnS dot is in the trion state with a lifetime of 1.1 ns at this range of potentials, which is close to the value from ensemble measurement. Since the energy transfer rate is much slower than trion decay, the lifetime of the trion is not affected. We presume that the lifetime for the doubly charged state cannot be resolved due to smaller PL signals and faster exciton decay.

We note that since the energy of 405 nm laser excitation is far above the band edge of CdSeS/ZnS, the absorbance of the dot in the neutral and charged state should remain constant. From -0.15 to -0.25 V, the PL intensity is about twice as high as that of the “off” state for the neutral dot, due to the dim emission of a negative trion state (Figure 6). It agrees well with the recent consensus that the trion is not dark enough to account for the “off” state.^{15,16} From the PL trace (Supporting Information, Figure S11) and histogram (Figure 6), there are fewer occurrences of the “off” state for voltages from 0 V to -0.35 V, which indicates that charging

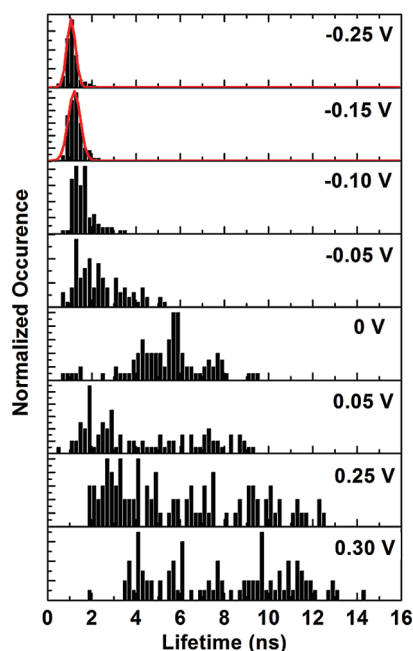


Figure 5. Histograms of the instantaneous lifetime at different voltages.

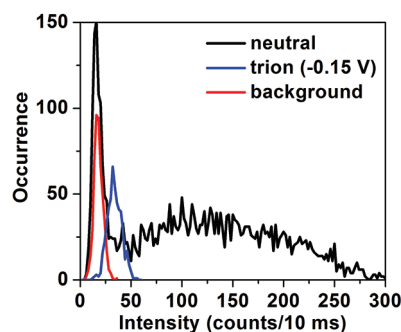


Figure 6. PL brightness histogram for a single CdSeS/ZnS dot at different potentials, indicating that the trion state is brighter than the “off” state.

helps suppress blinking as previously reported.²³ Especially, the dot shows no blinking events as long or longer than the bin width in the range from -0.15 to -0.25 V during the acquisition time, over which a single electron is injected. The PL intermittency returns when the reducing potential is removed. Blinking suppression has been reported by adding thiol moiety ligands³¹ or growing a thick CdS shell for CdSe nanocrystals.^{9,10} The injection of electrons into a single quantum dot might play a similar role as hole-scavenging ligands to passivate surface traps and prevent the surface from being oxidized by holes.

For CdSe/ZnS, the PL of single CdSe/ZnS QD can be also turned “on” and “off” reversibly under an external potential (Figure 7a). Similar to that of single CdSe/ZnS dots, the PL traces also sometimes present an intermediate intensity at -0.15 V, which would arise if fast single electron transfer occurs between the dot

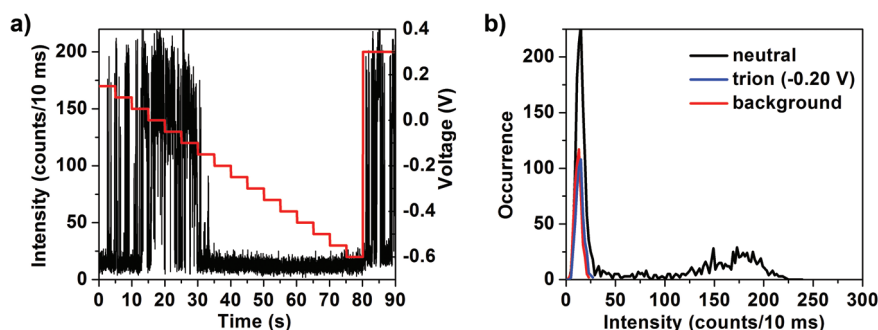


Figure 7. (a) PL trajectory of single CdSe/ZnS, varying applied voltage as shown. (b) PL brightness histogram for a single CdSe/ZnS dot at different potentials.

and substrate. Electron injection is confirmed by the appearance of a faster decay component in the lifetime traces as the voltage is brought to -0.15 V or above (Supporting Information, Figure S12). However, enhanced photon counts are not observed as the electron injection takes place, which indicates that the trion of single CdSe/ZnS is not bright enough to be observed. Indeed, the PL histogram (Figure 7b) shows that the signal for the single CdSe/ZnS dot at -0.20 V, the first voltage at which the neutral QD emission disappears, cannot be differentiated from the background and the “off” state. Therefore, the trion state of CdSe/ZnS is dimmer than that of CdSe/ZnS, confirming the slower trion decay rate for CdSe/ZnS QDs.³²

Most recently, we found that Galland *et al.* used the similar spectroelectrochemical control on single quantum dots to reveal the existence of two types of blinking mechanism.³³ However, they investigated the core–shell CdSe/CdS nanocrystals with thick shells (7–9 monolayers), the electron confinement of which is different from CdSe/ZnS alloyed nanocrystals in this discussion.

CONCLUSIONS

Electrochemical charging of single colloidal quantum dots (QDs) combined with spectroscopic studies has become a recent possibility.²³ In this work, small and photostable CdSeS/ZnS core/shell QDs were developed where the CdSeS core has an alloyed or gradient composition. For one specific size, these were then investigated as ensembles and as single dots to explore the difference on blinking and trion lifetime with CdSe/ZnS.

METHODS

Cadmium oxide (99.99%), oleic acid (90%), trioctylphosphine (90%), trioctylphosphine oxide (90%), zinc acetate (99.99%), hexamethyldisilathiane (synthesis grade), selenium (99.999%), and sulfur ($\geq 99.5\%$) were purchased from Sigma-Aldrich without further purification. All the preparations of stock solutions were performed in a nitrogen-filled glovebox. The stock solution for the precursors of CdSeS cores was prepared by dissolving sulfur (288.6 mg, 9.0 mmol) and selenium (16.6 mg, 0.21 mmol) in 10 mL of trioctylphosphine (TOP) under continuous

Ensemble measurements show that the biexciton recombination rate and the electron confinement energy are both smaller by $\sim 40\%$ in CdSeS/ZnS QDs, compared to CdSe/ZnS QDs with similar core size. However, PL lifetime measurements of ensembles under electrochemical control show that the trion decay rate of CdSeS/ZnS QDs is ~ 0.75 ns. In contrast, the trion lifetimes of the CdSe/ZnS dots is ~ 0.15 ns.

For single dots, the blinking behavior of CdSeS/ZnS shows a marginally larger exponent for the off-times, indicating only a slight suppression of blinking. The energy transfer mechanism between single QDs and the ITO substrate is confirmed by changing the film thickness of the ZnO spacer. Controllable charging at the single dot level was achieved by applying an electrochemical potential to single CdSeS/ZnS and CdSe/ZnS QDs, and the PL lifetimes were monitored by time-correlated photon counting with a pulsed excitation. Single CdSeS/ZnS dots exhibit a state with suppressed blinking that is brighter than the “off” state of a neutral dot or the background in our experiment. This state is assigned to the trion, and it has a resolved lifetime of ~ 1.1 ns in agreement with the ensemble results.

This work shows that ternary dot structures allow the achievement of longer trion lifetimes compared to binary dots of similar sizes. Long trion lifetimes and small quantum dots might present interesting possibilities for sensing and lasing. From a basic point of view, further investigations are needed to disentangle the observed correlation between the composition of the dots, the confinement energy, the density of states, and the Auger rate.

stirring. Zinc acetate ($\text{Zn}(\text{OAc})_2$) stock solution (0.50 mM) was made by dissolving $\text{Zn}(\text{OAc})_2$ (229.4 mg, 1.25 mmol) and trioctylphosphine oxide (TOPO, 0.5 g) in TOP (2.5 mL) at 80°C . Hexamethyldisilathiane ($(\text{TMS})_2\text{S}$) stock solution (0.50 mM) was made by adding $(\text{TMS})_2\text{S}$ (0.26 mL, 1.25 mmol) in TOP (2.5 mL). CdSe/ZnS QDs with an absorption edge at 595 nm were synthesized by adopting methods in earlier reports.²³ The fluorescence quantum yields of the nanocrystals were measured by comparison with a Rhodamine 6G solution in ethanol with the same optical density at the excitation wavelength. The absorbance for the band-edge transition is below 0.1, in order to minimize reabsorption.

Synthesis of CdSeS Alloyed Cores. The synthesis of CdSeS cores followed a previous report with small modifications.²¹ Typically, a flask of cadmium oxide (0.039 g, 0.3 mmol), oleic acid (0.38 mL, 1.2 mmol), and trioctylamine (6 mL) was heated to 100 °C for 20 min, under vacuum. After that, the flask was refilled with argon and then heated up to 300 °C. The high temperature was kept until a colorless solution was obtained. The mixture was cooled to 100 °C, and water was evaporated under vacuum. Filled with argon, the solution was reheated to 285 °C and a TOP solution (1 mL) of sulfur and selenium mixtures was injected swiftly. The temperature dropped to 280 °C and was maintained for 4 min, after which the solution was cooled to room temperature, preventing further growth of the alloyed quantum dots. This gave CdSeS cores of 5.0 ± 0.4 nm diameter with an absorption edge at 550 nm.

Synthesis of ZnS Shell on CdSeS Alloyed Cores. CdSeS cores in the 5 mL raw solution were precipitated by adding ethanol and then redissolved in 2 mL of hexane. A flask containing 2 g of hexadecylamine and 2.5 g of TOPO was heated to 120 °C under vacuum for 20 min. Subsequently, the flask was refilled with argon, and the CdSeS hexane solution was injected. The hexane was evaporated under vacuum for 20 min. With argon, the solution was heated to 180 °C, and 0.2 mL of Zn(OAc)₂ and 0.2 mL of (TMS)₂S stock solutions were added alternately in small portions over 5 min. The solution was then heated to 200 °C after which the procedure of adding precursors was repeated. Finally, the solution was heated to 220 °C; 0.8 mL of each precursor was added in 10 min as before. The solution was kept under 220 °C for 5 min before cooling to room temperature.

Microscopy Setup. Time-correlated single photon counting experiments of single dot photoluminescence were performed with a homemade confocal microscope. The pulsed excitation source was a 405 nm laser diode (Hamamatsu) with a 45 ps pulse duration and a 5 MHz repetition rate. The PL of a single quantum dot was collected by an infinity corrected oil immersion objective (Olympus, N.A. 1.45, 60 \times). A 50:50 beam splitter was used to separate the PL signal for simultaneous collection on an APD (PerkinElmer) and CCD camera (Andor). To study blinking and exciton lifetime changes simultaneously, time-tagged, time-resolved (TTTR) measurements using high-speed electronics (PicoQuant PH 300) were performed on each single quantum dot. The raw TTTR data were processed using homemade software. Blinking trajectories were extracted by aggregating the detected photons into 10 ms bins. For the single dot lifetime, the traces were extracted by constructing a histogram of photon delays with respect to the pulsed source. The resolution for the lifetime traces is 0.128 ns. To extract an "instantaneous" lifetime over much shorter time bins of 50 ms, the photon delays were averaged. The resulting average was compared to the average predicted by a single-exponential model, solving for the time constant. However, since the averaging enhances the effect of uncorrelated dark counts, one needs to suppress dark counts in the instantaneous lifetime calculation. This was achieved by counting only the photons in the first 20 ns window, both in the data and the model.

To suppress the energy transfer between the small quantum dots and the ITO substrate, a ZnO film was utilized as a transparent spacer.²³ ZnO nanocrystals were synthesized as reported by Cozzoli *et al.*³⁴ Thin ZnO films were deposited on indium tin oxide (ITO) coated coverslips (SPI) from hexane/octane (9:1) solution and then cross-linked by treating with 1,7-diaminoheptane.²³ In this work, the procedure was repeated several times to acquire a smooth ZnO film as measured by atomic force microscopy, while remaining moderately thick (Supporting Information, Figure S10). The single quantum dot film was prepared by drop-casting a dilute hexane/octane (9:1) solution of nanocrystals on the ITO/ZnO coated coverslip. The ITO coated coverslip was the optical window and working electrode for an airtight electrochemical cell with a platinum counter-electrode and cadmium pseudoreference electrode.

Acknowledgment. This work was supported by the donors of the Petroleum Research Fund through Grant ACS-PRF 51312-ND10. R.A.S. was supported by a NSEG fellowship from the

U.S. Department of Defense, Air Force Office of Scientific Research, 32 CFR 168a.

Supporting Information Available: TEM images and size distributions, CCD images of single quantum dots, decay curves for biexciton recombination, intraband absorption spectrum, PL trajectories and lifetime traces for single quantum dots under electrochemical control, AFM pictures of the morphology for ZnO films. This material is available free of charge via the Internet at <http://pubs.acs.org>.

REFERENCES AND NOTES

- Hines, M. A.; Guyot-Sionnest, P. Synthesis and Characterization of Strongly Luminescing ZnS-Capped CdSe Nanocrystals. *J. Phys. Chem.* **1996**, *100*, 468–471.
- Michalet, X.; Pinaud, F. F.; Bentolila, L. A.; Tsay, J. M.; Doose, S.; Li, J. J.; Sundaresan, G.; Wu, A. M.; Gambhir, S. S.; Weiss, S. Quantum Dots for Live Cells, *in Vivo* Imaging, and Diagnostics. *Science* **2005**, *307*, 538–544.
- Medintz, I. L.; Uyeda, H. T.; Goldman, E. R.; Mattoussi, H. Quantum Dot Bioconjugates for Imaging, Labelling and Sensing. *Nat. Mater.* **2005**, *4*, 435–446.
- Coe, S.; Woo, W.; Bawendi, M. G.; Bulovic, V. Electroluminescence from Single Monolayers of Nanocrystals in Molecular Organic Devices. *Nature* **2002**, *420*, 800–803.
- Anikeeva, P. O.; Halpert, J. E.; Bawendi, M. G.; Bulovic, V. Electroluminescence from a Mixed Red-Green-Blue Colloidal Quantum Dot Monolayer. *Nano Lett.* **2007**, *7*, 2196–2200.
- Kuno, M.; Fromm, D. P.; Hamann, H. F.; Gallagher, A.; Nesbitt, D. J. Nonexponential 'Blinking' Kinetics of Single CdSe Quantum Dots: A universal power law behavior. *J. Chem. Phys.* **2000**, *112*, 3117–3120.
- Kuno, M.; Fromm, D. P.; Hamann, H. F.; Gallagher, A.; Nesbitt, D. J. "On"/"Off" Fluorescence Intermittency of Single Semiconductor Quantum Dots. *J. Chem. Phys.* **2001**, *115*, 1028–1040.
- Margolin, G.; Protasenko, V.; Kuno, M.; Barkai, E. Power-Law Blinking Quantum Dots: Stochastic and Physical Models. *Adv. Chem. Phys.* **2006**, *133*, 327–356.
- Mahler, B.; Spinicelli, P.; Buil, S.; Quelin, X.; Hermier, J. P.; Dubertret, B. Towards Nonblinking Colloidal Quantum Dots. *Nat. Mater.* **2008**, *7*, 659–664.
- Chen, Y.; Vela, J.; Htoon, H.; Casson, J. L.; Werder, D. J.; Bussian, D. A.; Klimov, V. I.; Hollingsworth, J. A. "Giant" Multishell CdSe Nanocrystal Quantum Dots with Suppressed Blinking. *J. Am. Chem. Soc.* **2008**, *130*, 5026–5027.
- Wang, X.; Ren, X.; Kahen, K.; Hahn, M. A.; Rajeswaran, M.; Maccagnano-Zacher, S.; Silcox, J.; Cragg, G. E.; Efron, A. L.; Krauss, T. D. Nonblinking Semiconductor Nanocrystals. *Nature* **2009**, *459*, 686–689.
- Efron, A. L.; Rosen, M. Random Telegraph Signal in the Photoluminescence Intensity of a Single Quantum Dot. *Phys. Rev. Lett.* **1997**, *78*, 1110–1113.
- Nirmal, M.; Dabbousi, B. O.; Bawendi, M. G.; Macklin, J. J.; Trautman, J. K.; Harris, T. D.; Brus, L. E. Fluorescence Intermittency in Single Cadmium Selenide Nanocrystals. *Nature* **1996**, *383*, 802–804.
- Wang, C.; Shim, M.; Guyot-Sionnest, P. Electrochromic Nanocrystal Quantum Dots. *Science* **2001**, *291*, 2390–2392.
- Jha, P. P.; Guyot-Sionnest, P. Trion Decay in Colloidal Quantum Dots. *ACS Nano* **2009**, *3*, 1011–1015.
- Zhao, J.; Nair, G.; Fisher, B. R.; Bawendi, M. G. Challenge to the Charging Model of Semiconductor-Nanocrystal Fluorescence Intermittency from Off-State Quantum Yields and Multiexciton Blinking. *Phys. Rev. Lett.* **2010**, *104*, 157403.
- De-Rougemont, F.; Frey, R.; Roussignol, P.; Ricard, D.; Flytzanis, C. Evidence of Strong Auger Recombination in Semiconductor-Doped Glasses. *Appl. Phys. Lett.* **1987**, *50*, 1619–1621.
- Robel, I.; Gresback, R.; Kortshagen, U.; Schaller, R. D.; Klimov, V. I. Universal Size-Dependent Trend in Auger Recombination in Direct-Gap and Indirect-Gap Semiconductor Nanocrystals. *Phys. Rev. Lett.* **2009**, *102*, 177404–1.

19. Cragg, G. E.; Efron, A. L. Suppression of Auger Processes in Confined Structures. *Nano Lett.* **2009**, *10*, 313–317.
20. Garcia-Santamaria, F.; Brovelli, S.; Viswanatha, R.; Hollingsworth, J. A.; Htoon, H.; Crooker, S. A.; Klimov, V. I. Breakdown of Volume Scaling in Auger Recombination in CdSe/CdS Heteronanocrystals: The Role of the Core–Shell Interface. *Nano Lett.* **2011**, *11*, 687–693.
21. Jang, E.; Jun, S.; Pu, L. High Quality CdSeS Nanocrystals Synthesized by Facile Single Injection Process and Their Electroluminescence. *Chem. Commun.* **2003**, 2964–2965.
22. Swafford, L. A.; Weigand, L. A.; Bowers, M. J.; McBride, J. R.; Rapaport, J. L.; Watt, T. L.; Dixit, S. K.; Feldman, L. C.; Rosenthal, S. J. Homogeneously Alloyed CdS_{1-x}Se_x Nanocrystals: Synthesis, Characterization, and Composition/Size-Dependent Band Gap. *J. Am. Chem. Soc.* **2006**, *128*, 12299–12306.
23. Jha, P. P.; Guyot-Sionnest, P. Electrochemical Switching of the Photoluminescence of Single Quantum Dots. *J. Phys. Chem. C* **2010**, *114*, 21138–21141.
24. Embden, J. V.; Jasieniak, J.; Mulvaney, P. Mapping the Optical Properties of CdSe/CdS Heterostructure Nanocrystals: The Effects of Core Size and Shell Thickness. *J. Am. Chem. Soc.* **2009**, *131*, 14299–14309.
25. Li, J. J.; Wang, Y. A.; Guo, W.; Keay, J. C.; Mishima, T. D.; Johnson, M. B.; Peng, X. G. Large-Scale Synthesis of Nearly Monodisperse CdSe/CdS Core/Shell Nanocrystals Using Air-Stable Reagents via Successive Ion Layer Adsorption and Reaction. *J. Am. Chem. Soc.* **2003**, *125*, 12567–12575.
26. Pandey, A.; Guyot-Sionnest, P. Intraband Spectroscopy and Band Offsets of Colloidal II–VI Core/Shell Structures. *J. Chem. Phys.* **2007**, *127*, 104710.
27. A triexponential decay is convoluted with the IRF to fit the trion decay trace of CdSe/ZnS ensembles, with the lifetimes 0.1 (89%), 0.4 (11%), 30 (0.3%). The longest lifetime (30 ns) is attributed to the residue of lifetime decay of neutral dots. The same strategy was applied to fit the trion decay trace of CdSeS/ZnS ensembles, with lifetimes 0.55 (87%) and 2.1 ns (13%). The trion lifetimes were estimated as the weighted averages.
28. Jha, P. P.; Guyot-Sionnest, P. Photoluminescence Switching of Charged Quantum Dot Films. *J. Phys. Chem. C* **2007**, *111*, 15440–15445.
29. Fisher, B. R.; Eisler, H.; Stott, N. E.; Bawendi, M. G. Emission Intensity Dependence and Single-Exponential Behavior in Single Colloidal Quantum Dot Fluorescence Lifetimes. *J. Phys. Chem. B* **2003**, *108*, 143–148.
30. Brokmann, X.; Coolen, L.; Dahan, M.; Hermier, J. P. Measurement of the Radiative and Nonradiative Decay Rates of Single CdSe Nanocrystals through a Controlled Modification of their Spontaneous Emission. *Phys. Rev. Lett.* **2004**, *93*, 107403.
31. Hohng, S.; Ha, T. Near-Complete Suppression of Quantum Dot Blinking in Ambient Conditions. *J. Am. Chem. Soc.* **2004**, *126*, 1324–1325.
32. More PL traces of single CdSeS/ZnS and CdSe/ZnS quantum dots under electrochemical control are displayed in the Supporting Information.
33. Galland, C.; Ghosh, Y.; Steinbruck, A.; Sykora, M.; Hollingsworth, J. A.; Klimov, V. I.; Htoon, H. Two Types of Luminescence Blinking Revealed by Spectroelectrochemistry of Single Quantum Dots. *Nature* **2011**, *479*, 203–207.
34. Cozzoli, P. D.; Curri, M. L.; Agostiano, A.; Leo, G.; Lomascolo, M. ZnO Nanocrystals by a Non-hydrolytic Route: Synthesis and Characterization. *J. Phys. Chem. B* **2003**, *107*, 4756–4762.